Estimating the state of charge of lithium-ion batteries using different noise inputs

Anas El Maliki[1], Kamal Anoune[2], Abdessamad Benlafkih[3], Abdelkader Hadjoudja[1]
[1]Laboratory of Electronic Systems, Information Processing, Mechanics and Energetics, Faculty of Sciences,
University Ibn Tofail, Kenitra, Morocco
[2]SmartiLab EMSI, Honoris United Universities, Rabat, Morocco
[3]Advanced Systems Engineering Laboratory, National School of Applied Sciences, Ibn Tofail University, Kenitra, Morocco

Article Info

ABSTRACT

State of charge estimation (SOC) is the most significant functionality of a vehicle's battery management system (BMS). The methods for this estimation are conventionally oriented towards model-based methods. As part of this paper, we introduce a first order equivalent circuit estimation approach known as the Thevenin model, along with an extended Kalman filter (EKF) approach to accurately estimate the SOC. We then deploy and simulate it in MATLAB by using a reference load profile from the new European driving cycle (NEDC). Afterwards, the simulation results are reviewed based on various initial noise values, and the results are compared to those of other EKF algorithms. According to the results, SOC estimation accuracy has significantly increased as a result of the improvements made. Specifically, the root-mean-square error decreased from 0.0068 to 0.0020.

Corresponding Author:

Anas El Maliki
Laboratory of Electronic Systems, Information Processing, Mechanics and Energetics
Faculty of Sciences, University Ibn Tofail
Kenitra, Morocco
Email: anas.elmaliki@uit.ac.ma

1. INTRODUCTION

With the growth of public demand and government support, technological development strongly encouraged the use of electric vehicles. Lithium-ion batteries (LIBs) are drawing more research interest due to their environmental friendliness, higher energy density, higher power output, and longer lifespan [1], [2]. Vehicles that are powered by new energy sources are commonly equipped with LIBs. Therefore, obtaining an accurate battery state of charge (SOC) estimate becomes a challenging task for safe battery operation [3], [4]. The estimation of the SOC inside the battery management system (BMS) has the potential to enhance both the reliability and efficiency of the system. However, estimating SOC is significantly influenced by complicated factors related to self-discharge, discharge current, and battery aging, which leads to an imprecise estimation of SOC [5].

Currently, several approaches have emerged to estimate battery SOC. In general, the ampere-hour know as AH method is commonly employed because of its ease of implementation [6]. However, in practical application, this method is susceptible to errors caused by noise and random interference which tend to accumulate. As a result, various model-based algorithms have been proposed to correct those random errors.

The model-based methods provide a consistent performing method, like an equivalent circuit model, such as employing an equivalent circuit model in combination with state estimation computations. Among these methods, the Kalman filter is the commonly employed model. Nevertheless, the linear Kalman filter

(LKF) [7], [8] an only be applied to simple linear systems. To address nonlinear system applications, recent research has led to the development of extensions to the Kalman filter. In particular, the extended Kalman filter (EKF) [9], unscented Kalman filter (UKF) [10], and cubature Kalman filter (CKF) [11]. Utilizing the EKF can reduce the time to convergence in SOC estimation, yet it amplifies the computing burden on the battery management system (BMS) [12]. Fang *et al.* [13] suggested an iterative EKF method to estimate the SOC, which has shown improvements. However, the algorithm's robustness is limited when identifying and updating parameters such as battery capacity or internal resistance. Xiong *et al.* [14] employed an EKF approach to assess the SOC in a vanadium redox flow battery. The method uses measurement of applied currents and terminal voltages to predict the SOC, achieving a maximum error of 5.5% in SOC estimation. Sun *et al.* [15] and Tian *et al.* [16] proposed a novel approach to improve the accuracy of SOC estimation by integrating the first-order resistor-capacitor (RC) equivalent model with the EKF. They reported that this approach reduced the root mean square error (RMSE) of SOC estimation by 43.34 while only slightly increasing computational time by 4.59%.

The assessment of the EKF performance depends roughly on the key parameters Q and R, indeed Wang *et al.* [17] and Zhao *et al.* [18] show that picking these values provide a big challenge as the determination of the noise remains random and difficult. However, these values impact significantly on the estimation error and the convergence rate of the EKF process. The major contribution of this paper is to evaluate how the Q and R matrices influence the EKF estimation.

In this work, we proposed a method for estimating SOC using an extended Kalman filter in combination with the Thevenin battery model. Additionally, we present and discuss the implementation of the EKF using the MATLAB software. Moreover, we utilize the new European driving cycle (NEDC) [19] as a load profile for online SOC estimation. The organization of this paper is as follows: i) Section 2 provides details of the mathematical modeling of the Lithium-ion battery and its parameter identification method used; ii) Followed by a demonstration of the state-of-charge estimation method employed; iii) Section 3 presents the proposed method deployed on a MATLAB Simulink program, along with a discussion of the simulation data; iv) In section 4, we discuss the results obtained from the previous section; and v) Section 5 presents the conclusion.

2. MATHEMATICAL MODEL

2.1. Lithium-ion battery model

The most common battery models are electrochemical models (EM) and equivalent circuit models (ECM). An electrochemical model can be used to characterize external characteristics as well as to simulate changes in distribution and internal characteristics. Any physical meaning that can be attributed to a process can be represented by these changes. Nonetheless, since the electrochemical parameters and partial differential equations require considerable amounts of computation, electrochemical models are not commonly used in practice to assess the reliability of estimates of SOC. Equivalent circuit models, on the other hand, are more widely used for this purpose.

An equivalent circuit model represents a battery's external properties using hardware circuit elements like capacitors, resistors, and current loads. Due to their ease of use, these models are widely used to simulate battery performance. One of the most popular equivalent circuit models used is Thevenin model. Thevenin model shown in Figure 1 consists of voltage source a parallel RC circuit and a rint model. The main concept behind using Thevenin model is to characterize the battery's behavior by representing it with an equivalent resistance in series and a voltage source. The Thevenin model allows for better characterization of the dynamic properties of the battery compared to simpler models like rint model.
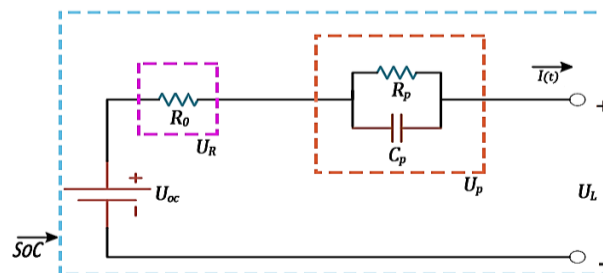

Figure 1. Thevenin battery model

In Figure, the terminal voltage and ohmic voltage are represented by U_L and U_R respectively. Here, R_0 stands for the internal resistance. The resistor-capacitor circuit, commonly referred to as the RC circuit, comprises both polarization resistance R_p and the polarization capacitance C_p. This circuit is utilized to illustrate the polarization effect exhibited by Li-ion batteries, with U_p indicating the polarization voltage. The Thevenin battery model equations are defined as (1), employing Kirchhoff's law for their derivation.

$$\begin{cases} U_L = U_{oc} - IR_0 - U_p \\ \dot{U}_p = -\frac{1}{C_p R_p} U_p + \frac{1}{C_p} I \end{cases} \tag{1}$$

2.2. Parameter identification

In this subsection, the hybrid pulse power characterization (HPPC) test and the recursive least square with forgetting factor (FFRLS) algorithms are conceived for the estimation of online battery parameters. The HPPC test is commonly used to determine the OCV-SOC relation. However, the test also provides a way to identify the parameter values from the ECM model which is derived from the offline parameter identification method [20], [21]. For performing the HPPC test, the outlined steps in Table 1, must be followed.

Table 1. HPPC test steps

Step	The test steps
Step 1	Keep the battery cell in a temperature control at 25 °C for four hours
Step 2	Load the cell with a constant current 1 C up to 4.2 V, then switch to a constant voltage 4.2 V until the current ≤ 0.05 C
Step 3	Give the cell a one hour rest
Step 4	Unload the cell with a current 1 C until 90% SOC. Wait until 1 hour, then discharge the cell at a current of 3 C for 10 s, put the cell to rest for 30s, then load it with a current 2.25 C for 10 s
Step 5	Now perform the same steps 4) for various SOC (80%, 70%..., 10%)

As a result, we adopt a sextic polynomial as a fit to the relation. Using $k_0 \sim k_6$ as a constants, as (2).

$$V_{ocv} = k_0 + k_1 Soc + k_2 Soc^2 + k_3 Soc^3 + k_4 Soc^4 + k_5 Soc^5 + k_6 Soc^6 \tag{2}$$

On the other hand, the FFRLS is employed to determine the battery parameters. Generally, recursive least square (RLS) algorithms are derived from the least square (LS) algorithm, and the basic principle is given by (3). Based on the Thevenin model described in Figure 1, the transfer function of the battery impedance is given by the following electrical equation with respect to the Laplace domain as (3).

$$G(s) = \frac{U(s) - U_{oc}(s)}{I(s)} = -\left(R_0 + \frac{R_p}{1 + R_p C_p s} \right) \tag{3}$$

A bilinear transformation is used to map as (3) to the Z plane. The transformation is represented as (4).

$$G(s) = \frac{a_2 + a_3 z^{-1}}{1 - a_1 z^{-1}} \tag{4}$$

The model parameters can be obtained as (5).

$$\begin{cases} a_1 = \frac{\Delta t - 2R_p C_p}{\Delta t + 2R_p C_p} \\ a_2 = \frac{R_0 \Delta t + R_p \Delta t + 2R_0 R_p \Delta t}{\Delta t + 2R_p C_p} \\ a_3 = \frac{R_0 \Delta t + R_p \Delta t - 2R_0 R_p \Delta t}{\Delta t + 2R_p C_p} \end{cases} \tag{5}$$

$$\begin{cases} R_0 = \frac{a_2 - a_3}{1 - a_1} \\ R_p = \frac{a_2 + a_3}{1 + a_1} - \frac{a_2 - a_3}{1 - a_1} \\ C_p = \frac{(1 - a_1)\Delta t}{2(1 - a_1)R_p} \end{cases} \tag{6}$$

2.3. State of charge estimation methods by EKF

As a standard method of estimating the battery's system of cells, we commonly use the EKF method. Due to its model of a nonlinear system, its approximation can accurately estimate system states across a wide range of operations [22]. Using the EKF, you get first-order polynomial accuracy where both quadratic and higher order terms are discarded. In addition to improving the algorithm's ability to handle nonlinear systems, EKF also adds flexibility to the algorithm, further improvements are needed to handle complex state monitoring problems in practical applications such as Li-ion batteries.

In the scenario of estimating SOC with an extended Kalman filter, the linear equation for the state-space model is requested at every time point near the latest estimation of SOC. To implement the EKF equations, the battery model must first be obtained. The input signal in this case is the charge/discharge current while the output is the voltage of the battery. The discrete state-space battery model equation for a nonlinear system can be as (7).

$$\begin{aligned} x_{k+1} &= f(x_k, u_k) + d_k \\ y_k &= g(x_k, u_k) + s_k \end{aligned} \tag{7}$$

Let $f(x_k, u_k)$ represent the nonlinear state transition function, and $g(x_k, u_k)$ denote the nonlinear measurement function. Taking into account both the state equation and measurement noise, we can express (7) as (8).

$$\begin{aligned} x_{k+1} &= \hat{A}_k x_k + f(\hat{x}_k, u_k) - \hat{A}_k \hat{x}_k + d_k \\ y_k &= \hat{C}_k x_k + g(\hat{x}_k, u_k) - \hat{C}_k \hat{x}_k + s_k \end{aligned} \tag{8}$$

The state along with the output, is predicted via nonlinear battery models. At time step k, the nonlinear battery model is linearized through the predicted state $\hat{x}_k^-$ to obtain the matrices $\hat{A}_k$, $\hat{B}_k$, and $\hat{C}_k$. These matrices are used when calculating and updating the covariance matrix of the state estimation errors and Kalman gain. This process leads to the main purpose of predicting $\hat{x}_k^-$ and P_k^-,

$$\hat{x}_k^- = A\hat{x}_{k-1}^+ + Bu_{k-1} + w_k \tag{9}$$

$$P_k^- = AP_{k-1}A^T + Q \tag{10}$$

and the update process is as (11), (12), and (13).

$$K_k = P_k C(CP_k^- C^T + R) \tag{11}$$

$$\hat{x}_k^+ = \hat{x}_k^- + K_k(y_k - C\hat{x}_k^- - D) \tag{12}$$

$$P_k^+ = P_k^-(I - K_k C) \tag{13}$$

Where K_k represents the Kalman gain vector, R is the covariance matrix of the zero-mean Gaussian measurement noise v_k, Q is the covariance matrix of the zero-mean Gaussian process noise w_k, and P_k is the covariance matrix of the state estimation error.

3. METHOD

The proposed model consists of three parts, as illustrated in Figure 2. The first part is the data input, where the input data is initialized. The FFRLS algorithm and the HPPC test are considered to determine the initial values for variables k_0 to k_6 and (R_0, R_p, C_p) in the system. These values play a crucial role in predicting the load state. Moving on to the second part, known as the Thevenin model, it involves two sub-steps. In step A, the model estimates certain parameters. Then, in step B, the SOC-OCV calculation is performed, which estimates the terminal voltage defined by (1). The third part is the SOC estimation, where the EKF algorithm is utilized. This estimation process comprises two steps. First, the model calculates the predicted state and current state. Next, the process incorporates initial noises Q and R as inputs. Finally, the state filter determines the resulting estimated SOC value. Notably, the proposed MATLAB model's current profile is derived from the new European driving cycle (NEDC) [23]. These three interconnected parts work together to predict and estimate various parameters and the state of charge in the system under study.
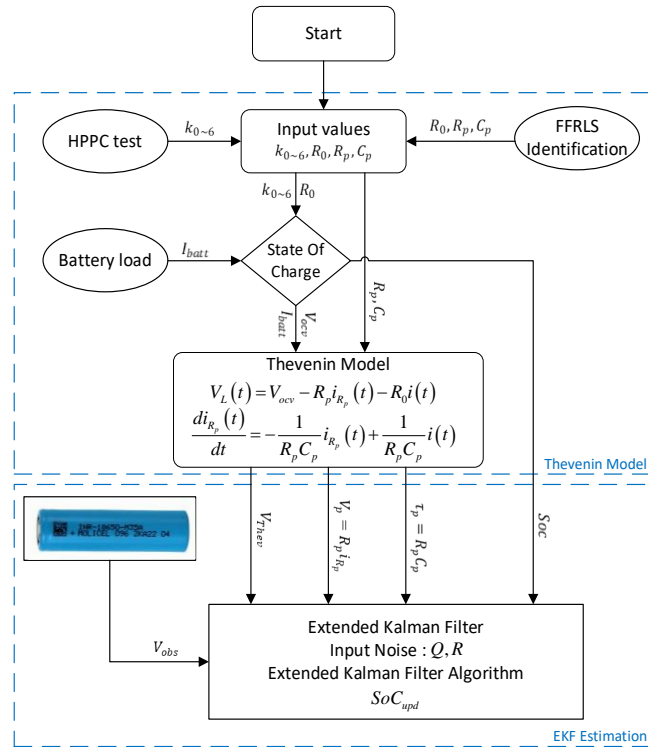
Figure 2. Flowchart of the proposed method

The NEDC current profile illustrated in Figure 3 has been used to construct the simulation of the battery using the proposed model. Based on the key parameters on both Tables 2 and 3, Figure 4 presents Thevenin model estimation of terminal voltage. Additionally, Figure 5 demonstrates the empirical model for estimating the state of charge. The HPPC test is conducted to gain the connection between OCV and SOC. The results obtained are fitted via a sixth-order polynomial with $k_{0\sim6}$ shown at Table 2 [24]. The system parameter identification is employed to obtain the parameter of the model on the basis of the SOC-OCV curve. Here the result of the parameters based on the FFRLS function is given in Table 3 [25].

Although the EKF estimation is adopted to estimate the SOC, their initial values of the Kalman parameters are determined as (14).

$$P_0 = \begin{bmatrix} 1e^{-1} & 0 \\ 0 & 1e^{-1} \end{bmatrix}, Q = \begin{bmatrix} Qa & 0 \\ 0 & Qb \end{bmatrix} = \begin{bmatrix} 2e^{-8} & 0 \\ 0 & 5e^{-3} \end{bmatrix}, R = 2e^{-1} \tag{14}$$

In accordance with (14), those values can be considered inputs to the EKF algorithm, as can be seen in Figure 6, which shows a comparison between the AH empirical method and the EKF SOC estimation of the NEDC test profile load for an electric vehicle, as well as Figure 7, which shows the respective errors of the methods.
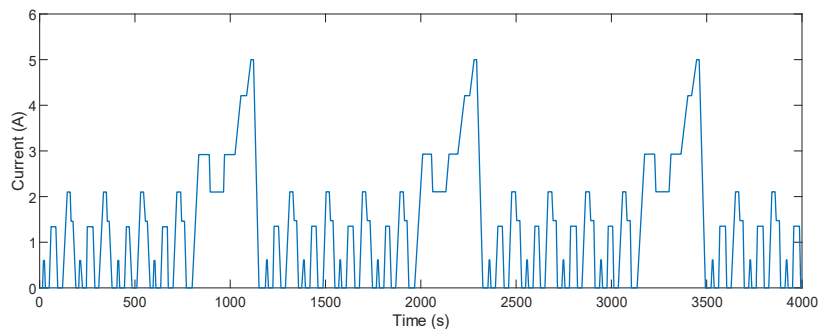

Figure 3. New European driving cycle (NEDC) load profile

Table 2. OCV-SOC fitting results at 25 °C						
k_0	k_1	k_2	k_3	k_4	k_5	k_6
3.353	2.478	−9.902	19.01	−14.44	2.351	1.319

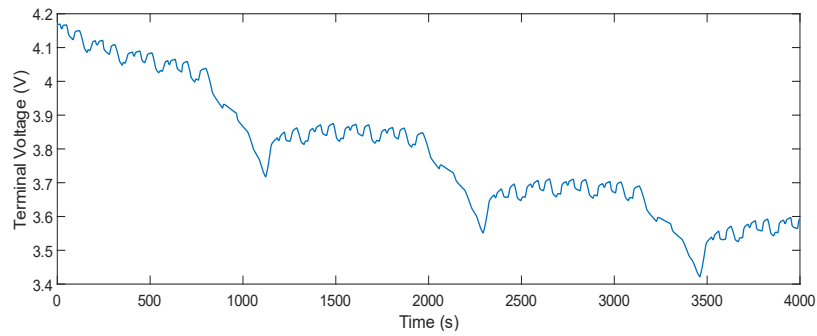| Table 3. Model parameters at 25 °C		
$R_0(\Omega)$	$R_P(\Omega)$	$C_P(F)$
0.0703	0.0481	750.6747

Figure 4. Terminal voltage using Thevenin model
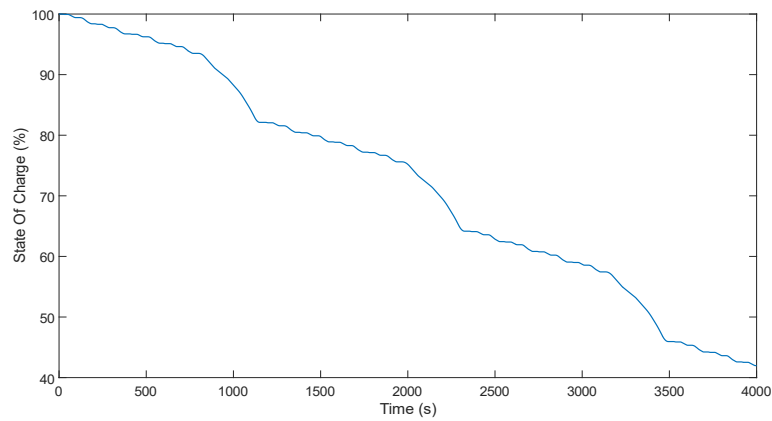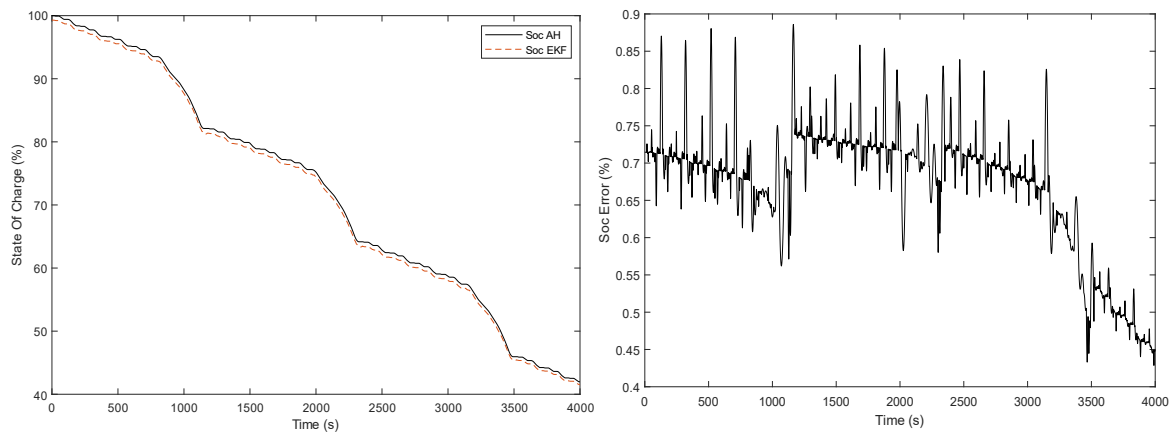

Figure 5. SOC Estimation using ampere-hour method

Figure 6. SOC Estimation results of the proposed model

Figure 7. SOC Estimation error results of the proposed model

4.   RESULT AND DISCUSSION

This section utilizes MATLAB/Simulink simulations to evaluate the proposed model under various parameters of the covariance matrix and compares it to the empirical ampere-hour (AH) model. According to

the proposed model, SOC results are influenced by three key parameters: i) Qa, ii) Qb, and iii) R. Additionally, two other parameters X and Y have a direct effect on these three key parameters. This relationship can be expressed as $Q_a = Xe^{-Y}$, and similarly for Qb and R, and vice versa.

4.1. Case 1: variation of Qa and Qb input noise parameters

In this case, the SOC was estimated using a parametric study. The R parameter is kept constant with a value of $R = 2e^{-1}$. To vary the input noise parameters, we use $Q_a = Xe^{-Y}$ and $Q_b = Xe^{-Y}$, where X and Y are subparameters that can be adjusted independently. The simulation of the EKF estimation using these parameters was performed under the NEDC load profile. The research aimed to evaluate the performance of the conventional EKF algorithm in estimating SOC for a specific system. The obtained results were presented in Figures 8 and 9, using the input values specified in Table 4. The analysis included comparisons between the estimated SOC values, as well as the corresponding errors introduced by the EKF algorithm.

To investigate the impact of the Y factor we conducted a comprehensive analysis by varying its values from 1 to 6. The results of this study were quite promising, as we observed in both Figures 8 and 9 a remarkable reduction in the maximum SOC estimation error. Initially recorded at 0.9778%, the error decreased significantly to 0.8971% as we made adjustments to the Y factor. This improvement in accuracy was further validated by a corresponding reduction in the RMSE, which dropped from 0.0075 to 0.0068. These findings demonstrate a substantial enhancement in the SOC estimation precision, underscoring the significance of the Y factor in refining the algorithm's performance.

Table 4. RMSE of SOC estimation under various Qa and Qb sub-parameters

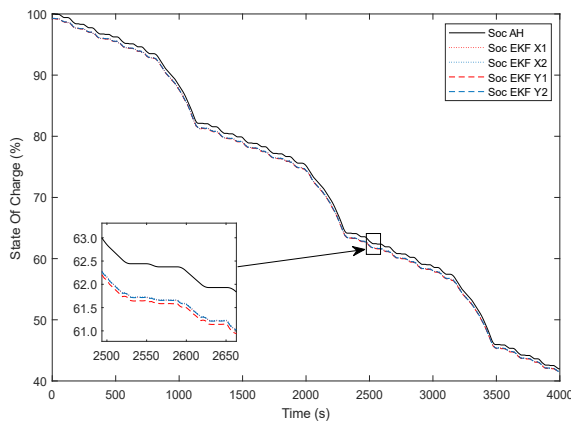|	Sub parameter X		Sub parameter Y	
	X_1	X_2	Y_1	Y_2
$Q_a = Xe^{-Y}$	$1e^{-8}$	$6e^{-8}$	$2e^{-1}$	$2e^{-6}$
$Q_b = Xe^{-Y}$	$1e^{-3}$	$6e^{-3}$	$5e^{-1}$	$5e^{-6}$
RMSE of EKF	0.0068	0.0068	0.0075	0.0068

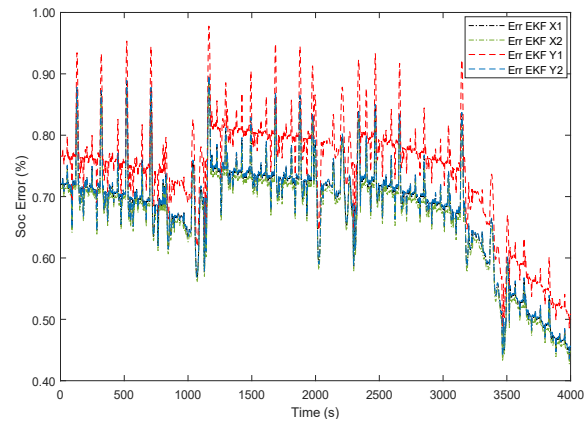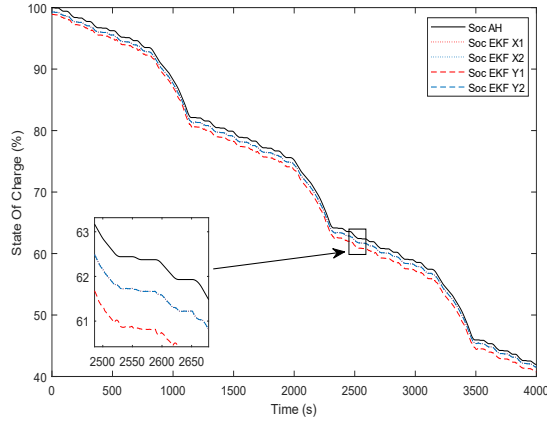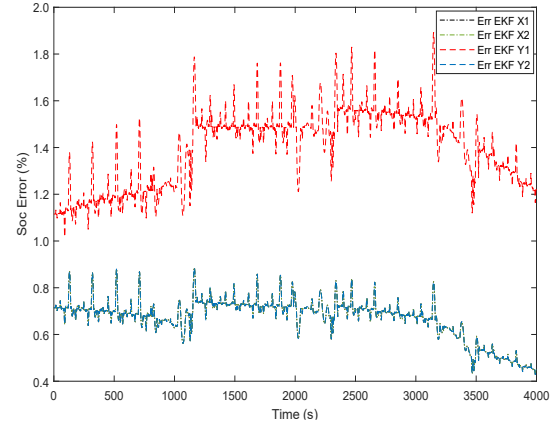Figure 8. SOC estimation results under varied sub-parameters X and Y of Qa & Qb

Figure 9. SOC estimation error results under varied sub-parameters X and Y of Qa & Qb

4.2. Case 2: variation of Qa input noise parameters

In this study, we estimation the SOC using a parametric study. The objective was to systematically investigate the system's behavior over a range of input parameters. For this example, we kept the parameters $Q_b = 5e^{-3}$ and $R = 2e^{-1}$ constant, while we varied the parameters X and Y of Q_a according to $Q_a = Xe^{-Y}$. Based on the input values specified in Table 5, we simulated the EKF estimation under the NEDS load profile. Figures 10 and 11 present the results obtained.

In this study, Figure 10 shows the measured and estimated SOC based on the input values provided in Table 5. Additionally, Figure 11 show the corresponding SOC errors. By comparing these results with other algorithms, it is evident that this algorithm produces a large error when $Q_a = 2e^{-1}$. However, by varying the Y factor between 1 and 4, we found that the maximum SOC estimation error was reduced from 1.8826% to 0.8856%, and the RMSE was reduced from 0.0140 to 0.0068.

Table 5. RMSE of SOC estimation under different Qa sub-parameters

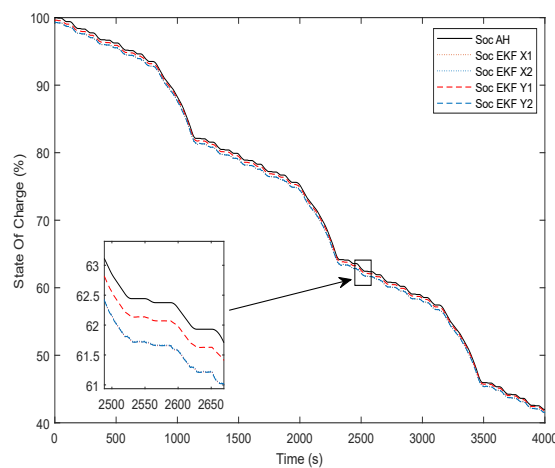|	Sub parameter X		Sub parameter Y	
	X_1	X_2	Y_1	Y_2
$Q_a = Xe^{-Y}$	$1e^{-8}$	$6e^{-8}$	$2e^{-1}$	$2e^{-4}$
RMSE of EKF	0.0068	0.0068	0.0140	0.0068

Figure 10. SOC estimation results under varied sub-parameters X and Y of Qa

Figure 11. SOC estimation error results under varied sub-parameters X and Y of Qa

4.3. Case 3: variation of Qb input noise parameters

Through a parametric study, an estimation of SOC was performed. In the following example, the $Q_a = 2e^{-8}$ and $R = 2e^{-1}$ parameter are kept constant, while X and Y sub parameters of $Q_b = Xe^{-Y}$ is varied. Using the parameters specified in Table 6, we simulated EKF estimation under the NEDS load profile. The results obtained are presented in Figures 12 and 13.

Table 6. RMSE of SOC estimation under different Qb sub-parameters

	Sub parameter X		Sub parameter Y	
	X_1	X_2	Y_1	Y_2
$Q_b = Xe^{-Y}$	$1e^{-3}$	$6e^{-3}$	$5e^{-1}$	$5e^{-6}$
RMSE of EKF	0.0068	0.0067	0.0030	0.0068

Figure 12. SOC estimation results under varied sub-parameters X and Y of Qb
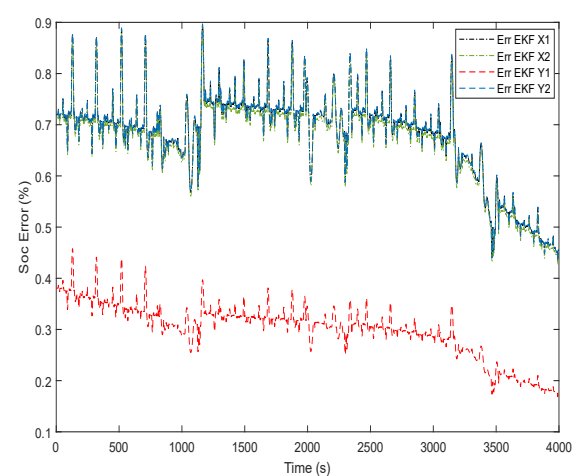

Figure 13. SOC estimation Error results under varied sub-parameters X and Y of Qb

According to Table 6, Figures 12 and 13 shows the measured and estimated SOC, along with the errors resulting from the conventional EKF algorithm. With $Q_b = 5e^{-1}$, this algorithm induces a very small error in comparison with other EKF algorithms. As a result of the Y factor being varied from 6 to 1, the maximum SOC estimation error has decreased from 0.8970% to 0.4554%, while the RMSE has decreased from 0.0068 to 0.0030.

4.4. Case 4: variation of R input noise parameters

A parametric study was conducted to estimate the SOC using the EKF method. In the following example, we kept the parameters $Q_a = 2e^{-8}$ and $Q_b = 5e^{-1}$ constant while varying the sub-parameters X and Y of $R = Xe^{-Y}$. These parameters were used as inputs in Table 7 to simulate the EKF estimation under a specific load profile known as the NEDS load profile. The results are shown in Figures 14 and 15.

The provided data in Table 7 serves as input values for the EKF algorithm, which is then illustrated in Figures 14 and 15. These figures represent both the measured and estimated SOC values, as well as the conventional EKF errors used for system evaluation. In comparison to other algorithms, this particular EKF algorithm shows a higher error of 0.5652% for $R = 5e^{-1}$. However, the error reduces significantly when the X factor is varied between 1 and 7. Specifically, the maximum error associated with SOC estimation decreases from 0.5051% to 0.3082%, and the RMSE reduces from 0.0034 to 0.0020. This improvement indicates the effectiveness of the EKF algorithm as the X factor is adjusted.

Table 7. RMSE of SOC estimation under different R sub-parameters

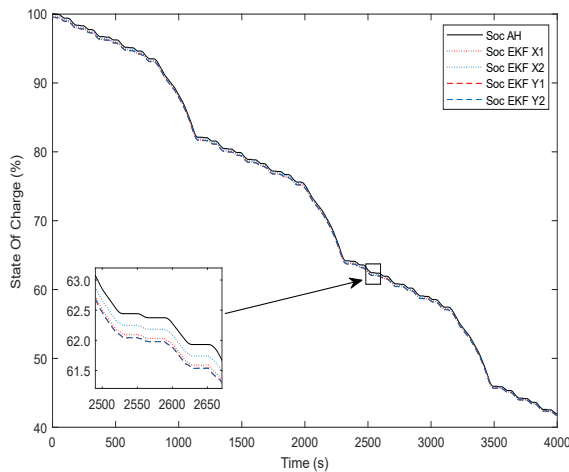|	Sub parameter X		Sub parameter Y	
	X_1	X_2	Y_1	Y_2
$R = Xe^{-Y}$	$1e^{-1}$	$7e^{-1}$	$2e^{-4}$	$2e^{-8}$
RMSE of EKF	0.0034	0.0020	0.0039	0.0039

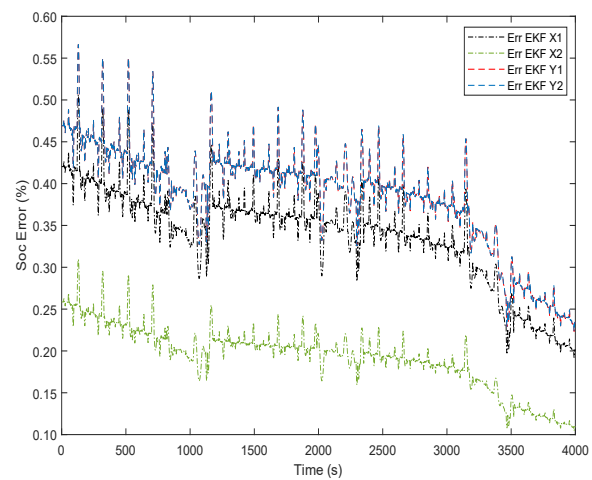Figure 14. SOC estimation results under varied sub-parameters X and Y of R

Figure 15. SOC estimation Error results under varied sub-parameters X and Y of R

5. CONCLUSION

To enhance the SOC estimation method's accuracy, we utilized the Thevenin model with an extended Kalman filter. Additionally, we introduced the new European driving cycle (NEDC) for testing purposes. The simulated data results demonstrate that our proposed model can predict SOC with a root mean square error (RMSE) of approximately 0.68%. During the implementation of the EKF algorithm, During the implementation of the EKF algorithm, we observed that the initial noise values of both the process covariance matrix Q and the measurement noise covariance matrix R significantly affect the state estimation process. To analyze this effect, we varied the initial noise matrices (Q and R) in MATLAB/Simulink. The comparative results indicate that the SOC estimation accuracy was notably improved, reducing the maximum SOC estimation error from 1.8826% to 0.3082%, and the RMSE from 0.0140 (1.4%) to 0.0020 (0.2%).

REFERENCES

[1] P. Shrivastava, T. K. Soon, M. Y. I. Bin Idris, and S. Mekhilef, "Overview of model-based online state-of-charge estimation using Kalman filter family for lithium-ion batteries," *Renewable and Sustainable Energy Reviews*, vol. 113, p. 109233, Oct. 2019, doi: 10.1016/j.rser.2019.06.040.

[2] F. Yang, Y. Xing, D. Wang, and K.-L. Tsui, "A comparative study of three model-based algorithms for estimating state-of-charge of lithium-ion batteries under a new combined dynamic loading profile," *Applied Energy*, vol. 164, pp. 387–399, Feb. 2016, doi: 10.1016/j.apenergy.2015.11.072.

[3] X. Xu, D. Wu, L. Yang, H. Zhang, and G. Liu, "State Estimation of Lithium Batteries for Energy Storage Based on Dual Extended Kalman Filter," *Mathematical Problems in Engineering*, vol. 2020, pp. 1–11, Apr. 2020, doi: 10.1155/2020/6096834.

[4] Y. Lin, X. Xu, F. Wang, and Q. Xu, "Active equalization control strategy of charge estimation of an electrochemical-thermal coupling model," *International Journal of Energy Research*, vol. 44, no. 5, pp. 3778–3789, Apr. 2020, doi: 10.1002/er.5166.

[5] C. Jin, "Brief Talk about Lithium-ion Batteries' Safety and Influencing Factors," *IOP Conference Series: Materials Science and Engineering*, vol. 274, p. 012152, Dec. 2017, doi: 10.1088/1757-899X/274/1/012152.

[6] K. Movassagh, A. Raihan, B. Balasingam, and K. Pattipati, "A Critical Look at Coulomb Counting Approach for State of Charge Estimation in Batteries," *Energies*, vol. 14, no. 14, p. 4074, Jul. 2021, doi: 10.3390/en14144074.

[7] P. Manoharan, M. R, K. K, and S. R, "SoC Estimation and Monitoring of Li-ion Cell using Kalman-Filter Algorithm," *Indonesian Journal of Electrical Engineering and Informatics (IJEEI)*, vol. 6, no. 4, p. 548, Dec. 2018, doi: 10.52549/ijeei.v6i4.548.

[8] J. Dou *et al.*, "Extreme learning machine model for state-of-charge estimation of lithium-ion battery using salp swarm algorithm," *Journal of Energy Storage*, vol. 52, p. 104996, Aug. 2022, doi: 10.1016/j.est.2022.104996.

[9] P. Venegas, D. Gómez, M. Arrinda, M. Oyarbide, H. Macicior, and A. Bermúdez, "Kalman filter and classical Preisach hysteresis model applied to the state of charge battery estimation," *Computers & Mathematics with Applications*, vol. 118, pp. 74–84, Jul. 2022, doi: 10.1016/j.camwa.2022.05.009.

[10] Y. Tian, B. Xia, W. Sun, Z. Xu, and W. Zheng, "A modified model based state of charge estimation of power lithium-ion batteries using unscented Kalman filter," *Journal of Power Sources*, vol. 270, pp. 619–626, Dec. 2014, doi: 10.1016/j.jpowsour.2014.07.143.

[11] J. Luo, J. Peng, and H. He, "Lithium-ion battery SOC estimation study based on Cubature Kalman filter," *Energy Procedia*, vol. 158, pp. 3421–3426, Feb. 2019, doi: 10.1016/j.egypro.2019.01.933.

[12] B. Li and C. Hu, "Multifunctional Estimation and Analysis of Lithium-Ion Battery State Based on Data Model Fusion under Multiple Constraints," *Journal of The Electrochemical Society*, vol. 169, no. 11, p. 110548, Nov. 2022, doi: 10.1149/1945-7111/aca2ee.

[13] H. Fang, Y. Wang, Z. Sahinoglu, T. Wada, and S. Hara, "State of charge estimation for lithium-ion batteries: An adaptive approach," *Control Engineering Practice*, vol. 25, pp. 45–54, Apr. 2014, doi: 10.1016/j.conengprac.2013.12.006.

[14] B. Xiong, J. Zhao, Z. Wei, and M. Skyllas-Kazacos, "Extended Kalman filter method for state of charge estimation of vanadium redox flow battery using thermal-dependent electrical model," *Journal of Power Sources*, vol. 262, pp. 50–61, Sep. 2014, doi: 10.1016/j.jpowsour.2014.03.110.

[15] D. Sun *et al.*, "State of charge estimation for lithium-ion battery based on an Intelligent Adaptive Extended Kalman Filter with improved noise estimator," *Energy*, vol. 214, p. 119025, Jan. 2021, doi: 10.1016/j.energy.2020.119025.

[16] X. Sun, X. Tang, X. Tian, J. Wu, and J. Zhu, "Position Sensorless Control of Switched Reluctance Motor Drives Based on a New Sliding Mode Observer Using Fourier Flux Linkage Model," *IEEE Transactions on Energy Conversion*, vol. 37, no. 2, pp. 978–988, 2022, doi: 10.1109/TEC.2021.3125494.

[17] W. Wang and J. Mu, "State of Charge Estimation for Lithium-Ion Battery in Electric Vehicle Based on Kalman Filter Considering Model Error," *IEEE Access*, vol. 7, pp. 29223–29235, 2019, doi: 10.1109/ACCESS.2019.2895377.

[18] L. Zhao, D. J. Thrimawithana, and U. K. Madawala, "Hybrid Bidirectional Wireless EV Charging System Tolerant to Pad Misalignment," *IEEE Transactions on Industrial Electronics*, vol. 64, no. 9, pp. 7079–7086, 2017, doi: 10.1109/TIE.2017.2686301.

[19] J. Chen, X. Feng, L. Jiang, and Q. Zhu, "State of charge estimation of lithium-ion battery using denoising autoencoder and gated recurrent unit recurrent neural network," *Energy*, vol. 227, p. 120451, Jul. 2021, doi: 10.1016/j.energy.2021.120451.

[20] Y. Wang *et al.*, "A comprehensive review of battery modeling and state estimation approaches for advanced battery management systems," *Renewable and Sustainable Energy Reviews*, vol. 131, p. 110015, Oct. 2020, doi: 10.1016/j.rser.2020.110015.

[21] J. C. D. Mushini, K. Rana, and M. S. Aspalli, "Analysis of open circuit voltage and state of charge of high power lithium ion battery," *International Journal of Power Electronics and Drive Systems (IJPEDS)*, vol. 13, no. 2, pp. 657–664, Jun. 2022, doi: 10.11591/ijpeds.v13.i2.pp657-664.

[22] R. P. Priya, S. R, and R. Sakile, "State of charge estimation of lithium-ion battery based on extended Kalman filter and unscented Kalman filter techniques," *Energy Storage*, vol. 5, no. 3, Apr. 2023, doi: 10.1002/est2.408.

[23] X. Lai, D. Qiao, Y. Zheng, and L. Zhou, "A Fuzzy State-of-Charge Estimation Algorithm Combining Ampere-Hour and an Extended Kalman Filter for Li-Ion Batteries Based on Multi-Model Global Identification," *Applied Sciences*, vol. 8, no. 11, p. 2028, Oct. 2018, doi: 10.3390/app8112028.

[24] Z. He *et al.*, "State-of-charge estimation of lithium ion batteries based on adaptive iterative extended Kalman filter," *Journal of Energy Storage*, vol. 39, p. 102593, Jul. 2021, doi: 10.1016/j.est.2021.102593.

[25] R. Xiao, Y. Hu, X. Jia, and G. Chen, "A novel estimation of state of charge for the lithium-ion battery in electric vehicle without open circuit voltage experiment," *Energy*, vol. 243, p. 123072, Mar. 2022, doi: 10.1016/j.energy.2021.123072.

BIOGRAPHIES OF AUTHORS

Anas El Maliki 🆔 📧 SC ⬡ received a B.S. degree in fundamental physics studies from Mohammed V University of Rabat in 2014 and an M.S. degree in physics and new technology from Hassan II University of Casablanca in 2017. He is currently working toward a Ph.D. degree in energy storage and sustainable energy at Ibn Tofail University, Kenitra. He can be contacted at email: anas.elmaliki@uit.ac.ma.

Kamal Anoune 🆔 📇 SC ↻ is currently a Research Professor at EMSI-Rabat, Honoris United Universities, he received his state engineering degree in electrical engineering in 2012, after he launched his start-up specializing in automation and renewable energy, his passion for knowledge in R&D led him to rejoint university in 2015 and obtained his Ph.D. degree in 2020 related to sizing-optimization of PV-wind-battery based micro-grid system. His current works are focused in smart grid, energy auditing, green hydrogen, and energy management opportunities. He can be contacted at email: kamal.anoune@gmail.com.

Abdessamad Benlafkih 🆔 📇 SC ↻ received the B.S. and M.S. degrees, from the University of Sciences Dhar El Mehraz Fez, In 1997 and 2003, respectively, and the Ph.D. degree in electrical engineering from the University Ibn Tofail Kenitra in 2015. He was a teacher in the secondary cycle from 2004 to 2020. In 2020, he has been a Professor of Electrical Power Engineering at University Ibn Tofail Kenitra Morocco. He can be contacted at email: abdessamad.benlafkih@uit.ac.ma

Abdelkader Hadjoudja 🆔 📇 SC ↻ was an engineer and was awarded a doctorate in microelectronic by the National Polytechnic Institute of Grenoble, France, in 1997. He worked for 6 years as PLD Leader Engineer Software in Atmel, Grenoble, France, and as a consultant within design and reuse. Since July 2010, he has been a full Professor of Electronics at Ibn Tofail University, Kenitra. He can be contacted at email: abdelkader.hadjoudja@uit.ac.ma.